

Effect of ageing on martensitic transformation in NiTi shape memory alloy

DANUTA STROZ, JERZY KWARCIAK, HENRYK MORAWIEC
*Silesian University, Institute of Physics and Chemistry of Metals, Bankowa 12,
 40-007 Katowice*

The shape memory effect in Ni-49 Ti alloy after solution treatment at 800° C for 0.5 h and ageing at 400, 500, 600 and 700° C for 1 h has been investigated by means of transmission electron microscopy and differential thermal analysis (DTA) measurement. Ageing at 400 and 500° C for 1 h causes the precipitation of characteristic temperatures towards higher values. In sample aged at 500° C three distinct DTA peaks arise giving evidence of intermediate stages of the martensite transformation.

1. Introduction

One of the methods for generating the two-way shape memory effect in NiTi alloys is by introducing fine particles which do not dissolve during the reverse martensitic transformation on heating [1, 2]. It is suggested that the spontaneous shape change is caused by the internal stress field arising around the precipitates and resulting in oriented growth of martensite plates. The crystal structure of the precipitates in nickel rich NiTi alloys aged at the temperature range of 300 to 500° C has been reported by other authors [3-6]. The latest results obtained [7] confirm that the precipitates have a rhombohedral structure and a composition of Ni₄Ti₃. The presence of the precipitates in the matrix can influence the reverse martensite transformation behaviour in the alloy [8]. The aim of this work was to examine the transformation sequences which occur in a nickel rich NiTi alloy after various ageing treatments.

2. Experimental procedure

The Ni-49 at % Ti alloy was prepared by melting in a high-frequency vacuum induction furnace. After casting, the ingots were homogenized at 870° C and hot rolled to strips of about 0.7 mm in thickness. Then the strips were annealed at 500° C for 0.5 h. The specimens were solution treated at 800° C for 0.5 h and then aged at 400, 500, 600 and 700° C for 1 h.

The microstructure of the specimens was observed by transmission electron microscope (TEM) in a JEM 200B operating at 200 kV. Thin foils for TEM were prepared by the jet polishing technique in a solution containing 20 vol % HClO₄ in CH₃COOH.

Differential thermal analysis (DTA) experiments were performed with a Mettler TA1 thermoanalyser. Heating and cooling runs from -50° C to 100° C were carried out in a helium atmosphere. Pure nickel was used as a standard.

3. Experimental results

3.1. The structure and transformation temperatures of the as-quenched alloy

The characteristic temperatures of the solution treated and quenched NiTi alloy were determined by DTA to be about $A_s = -32^\circ\text{C}$, $A_f = 6^\circ\text{C}$, $M_s = -40^\circ\text{C}$, $M_f = -65^\circ\text{C}$ (Fig. 1). On the DTA curves single peaks were observed both for martensite and reverse transformations. The microstructure of the alloy examined at room temperature exhibited only a few dislocations, and antiphase-like microdomains contrast associated with SRO in this alloy (Fig. 3). The ordered B2 structure was also revealed by electron diffraction, Figs 2b and c.

3.2. Effect of ageing temperatures

Ageing of the alloy has a significant effect on its characteristic temperatures and kinetics of the martensitic transformations as well as on the microstructure. The DTA curves during heating and cooling (Fig. 4a) of the samples aged at 400° C were similar to the quenched alloy but the characteristic temperatures had shifted towards higher values ($A_s = 5^\circ\text{C}$, $A_f =$

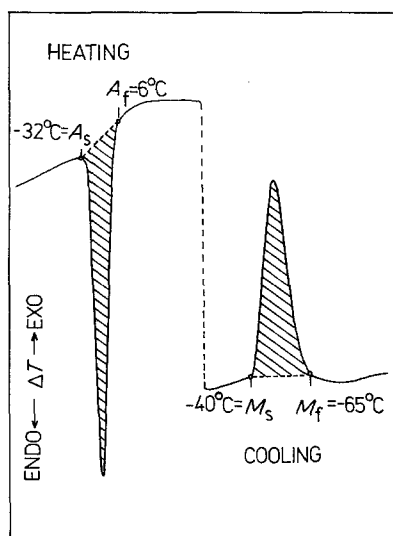


Figure 1 DTA curves for the quenched alloy (heating/cooling rates— 6°C min^{-1}).

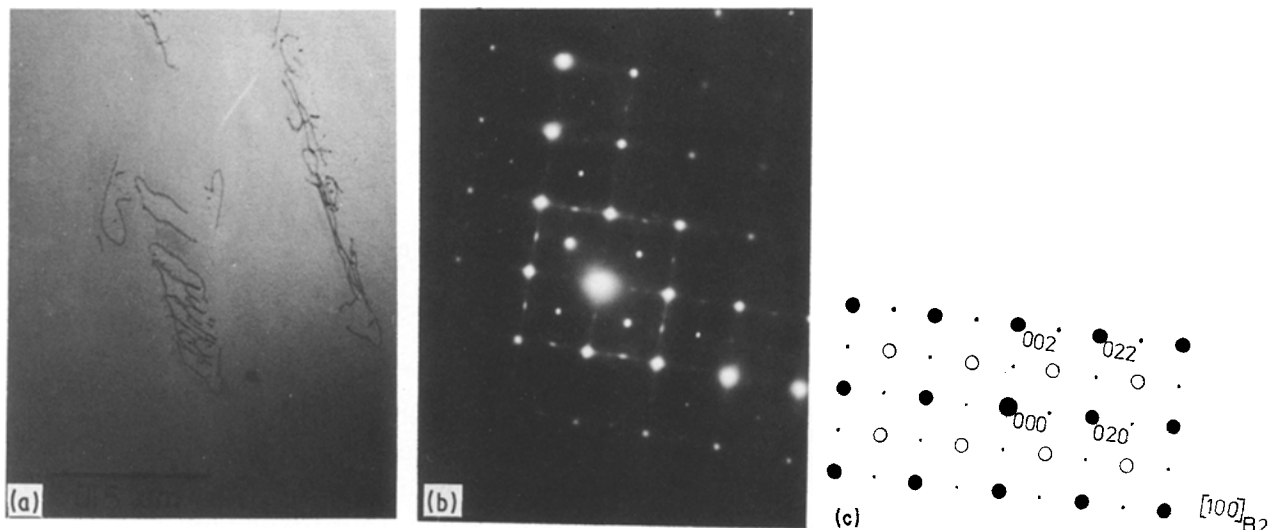


Figure 2 (a) The structure of the quenched alloy, (b) the diffraction pattern, (c) the indexed pattern.

50°C, $M_s = -15^\circ\text{C}$, $M_f = -50^\circ\text{C}$). The temperature ranges of transformations both during heating and cooling were slightly wider than in the as-quenched alloy. In the electron microscopy images small lenticular particles appear (Fig. 5). They were coherent with parent matrix and exhibited typical strain-field contrast. These particles grew significantly in samples aged at 500°C (Fig. 6), at which temperature the particles lost coherency. Their sizes were about 200 nm and their density in the parent matrix was high. In the literature data there is no concensus about

crystal structure and stoichiometry of these particles. Thus, to index the diffraction patterns we used a structure model of this phase introduced by Tadaki *et al.* [7]. They presumed that the investigated phase is of rhombohedral structure with $a = 0.670\text{ nm}$ and $\alpha = 113.8^\circ$ in which 14 atoms are involved and of stoichiometry of Ni_4Ti_3 . We calculated the interplanar distances and structural factors of the phase based on this model and also simulated some basic diffraction patterns. The experimental diffraction patterns were in good agreement with the calculated data (Fig. 7).

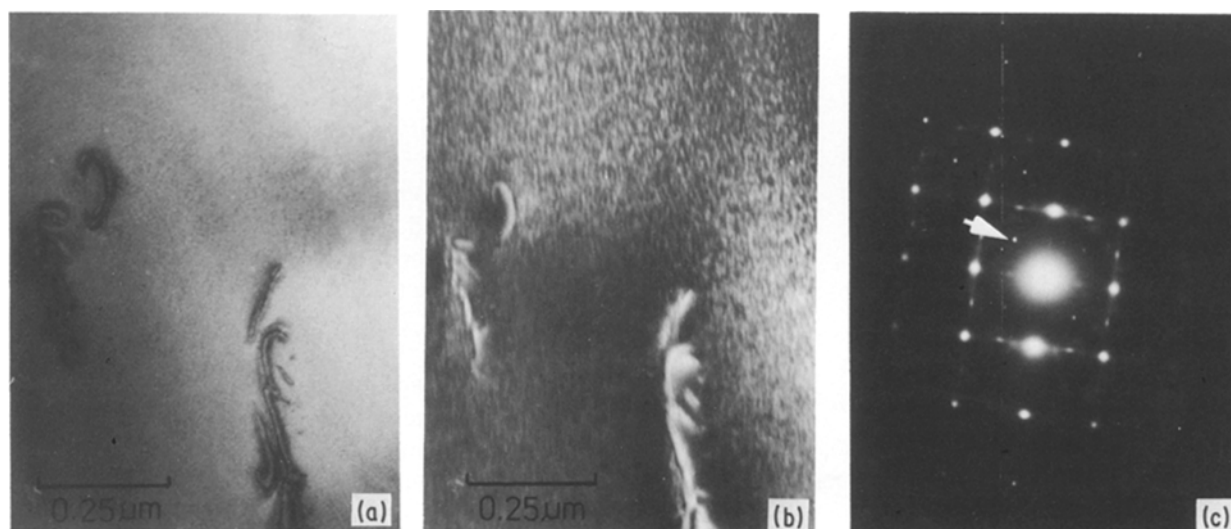


Figure 3 Antiphase-like microdomains contrast visible on the electron microscopic images (a) bright-field image, (b) dark-field image, (c) diffraction pattern from (a) (the arrow indicates the reflection from which the dark-field image was taken).

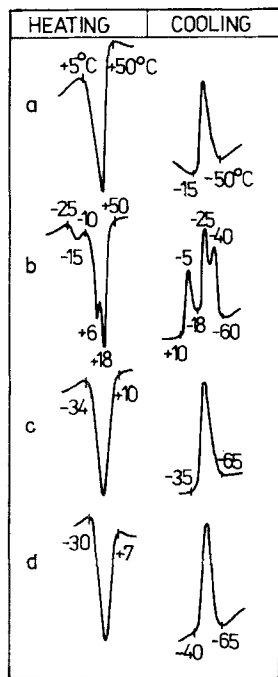


Figure 4 DTA curves for the alloy aged at (a) 400°C for 1 h, (b) 500°C for 1 h, (c) 600°C for 1 h, (d) 700°C for 1 h.

The effect of ageing at 500°C was also observed on the DTA curves. The samples aged at this temperature gave three distinct DTA peaks at -15°C, 6°C and 18°C during heating and -5°C, -25°C and -40°C

during cooling (Fig. 4b). This complicated character of the DTA curves was observed only for samples aged at 500°C. Increasing the ageing temperature to 600°C caused the single DTA peaks to return (Fig. 4c). In comparison with the samples aged at 400°C and 500°C the characteristic transformation temperatures decreased to values near to those obtained for the quenched alloy. Similar results were obtained for specimens aged at 700°C (Fig. 4d). Particles were not observed in the TEM after ageing at 600°C and 700°C (Fig. 8). The structure of these samples was quite similar to that of the quenched alloy, although the SRO effects were much larger.

4. Discussion

The structure of the as-quenched NiTi alloy is typical for the alloys of these compositions [3] i.e. at room temperature the alloy exhibits the ordered B2 phase. Ageing of the alloy at 400°C and 500°C caused precipitation of nickel-rich phase (Ni_4Ti_3). This results in the decrease of nickel content and the increase of internal stress fields in the matrix. These two factors should act in opposition. The decrease of nickel content causes an increase of M_s temperature [9], while the stress field formed around precipitates suppresses the martensitic transformation [8]. In the case of the alloy studied the martensitic transformation temperatures increased significantly for specimens aged at 400°C and 500°C in comparison with the quenched alloy. It

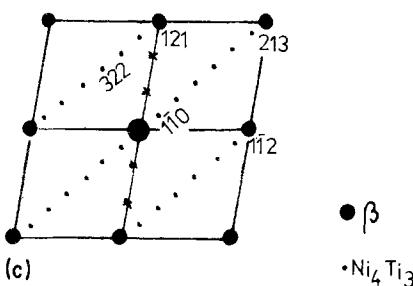
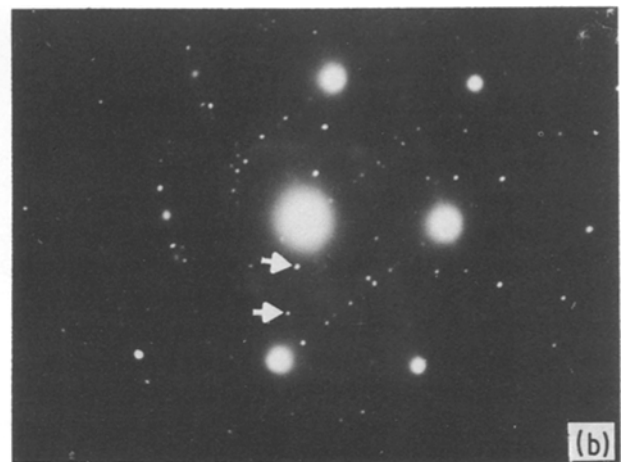
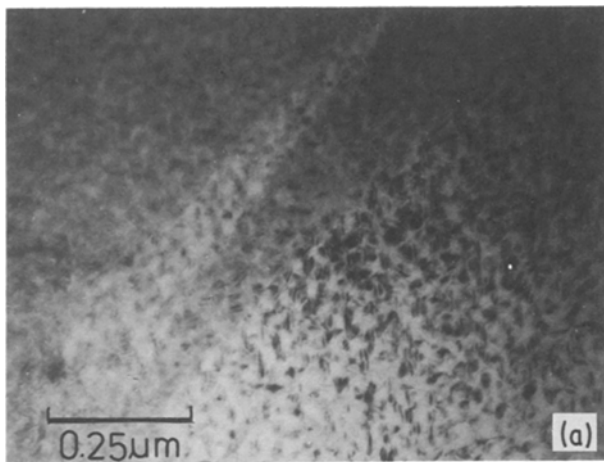


Figure 5 (a) The structure of the alloy aged at 400°C for 1 h, (b) the diffraction pattern (arrows indicate the reflections from R-phase) and (c) the indexed diffraction pattern.

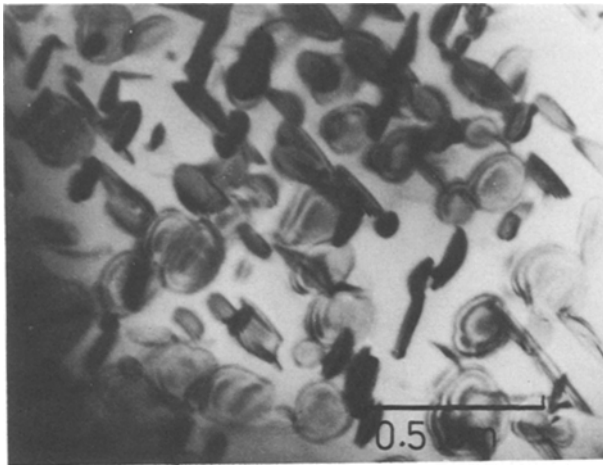


Figure 6 Lamellar particles in the alloy aged at 500°C for 1 h.

can be suggested that the decrease of nickel content in the matrix played the main role in the change observed on the DTA curves. There are no precipitates in samples aged at 600°C and 700°C. Thus, the reverse martensitic transformation is responsible for the single peaks on the DTA curve obtained for these

samples. After ageing at 500°C three distinct DTA peaks were registered. It is difficult to interpret them unambiguously. According to [10] after solution treatment and ageing the transformation sequence in nickel-rich NiTi alloys can be as follows: $M \leftrightarrow R \leftrightarrow B_2$. However, in the alloy aged at 400°C and 500°C nickel-

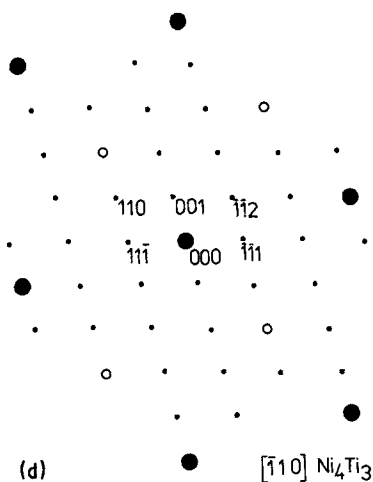
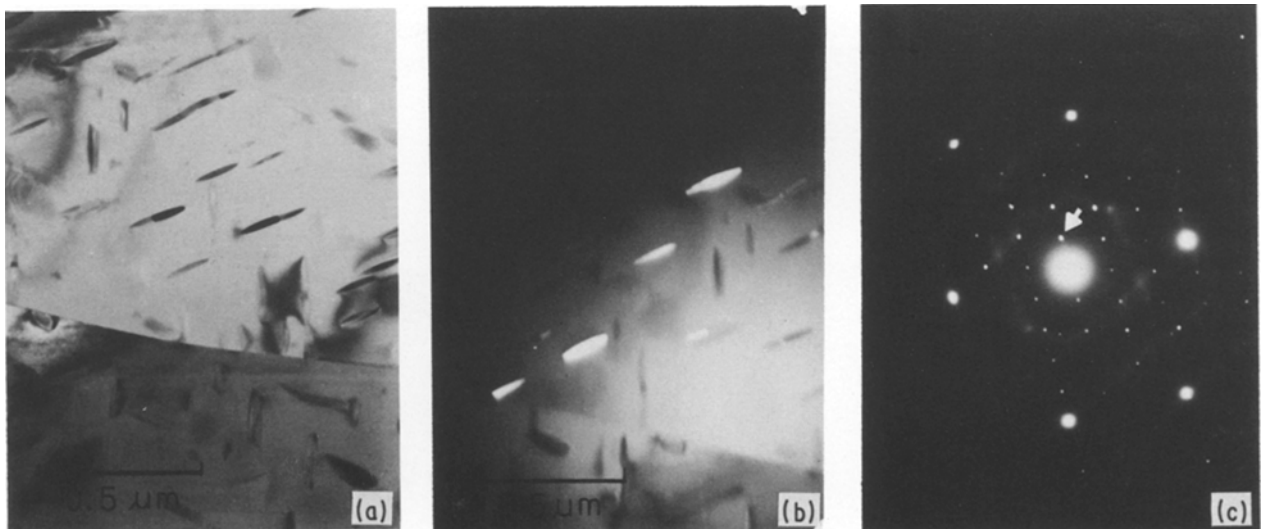


Figure 7 Particles of Ni_4Ti_3 phase in the alloy aged at 500°C for 1 h (a) bright-field image, (b) dark-field image, (c) diffraction pattern from the area (a) (the arrow indicates the reflection in which the dark-field image was taken) (d) indexed electron diffraction pattern (c).

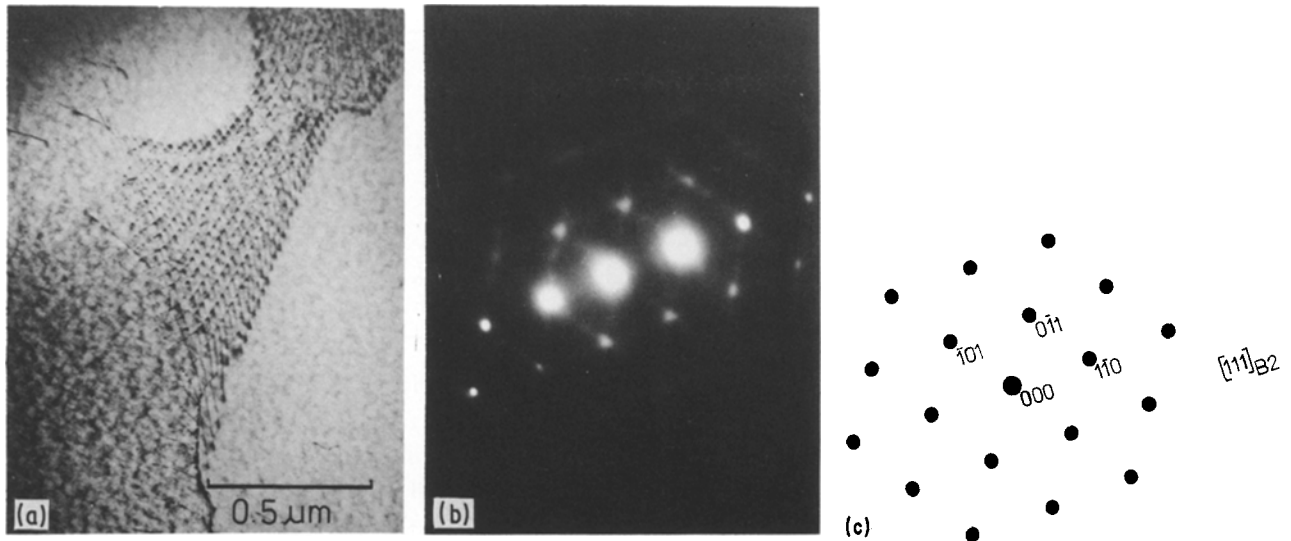


Figure 8 The structure of the alloy aged at 600°C for 1 h.

rich precipitates were observed. This causes a decrease in the nickel content of the matrix so that it approaches the near equiatomic composition. For alloys of this composition the following sequence of the transformations has been reported: $B2 \rightarrow B2 + B19' \rightarrow R + B19' \rightarrow B19'$ [8, 11]. This sequence can explain the occurrence of the three peaks on the DTA curves (Fig. 4b). Thus the first peak could be due to presence of a small amount of $B19'$ phase, then the parent phase transforms to the R phase (the second DTA peak) and in the last stage the R phase transforms into martensitic $B19'$ phase (the third DTA peak).

References

1. R. OSHIMA and E. NAYA, *J. Jpn Inst. Met.* **42** (1978) 463.
2. M. NISHIDA and T. HONMA, *Scripta Metall.* **18** (1984) 1293.
3. M. NISHIDA, C. M. WAYMAN and T. HONMA, *ibid.* **18** (1984) 1389.
4. *Idem, ibid.* **19** (1985) 938.
5. D. KOSKIMAKI, M. J. MARCINKOWSKI and A. S. SASTRI, *Trans. Met. Soc. AIME* **245** (1969) 1883.
6. S. P. GUPTA, K. MUKHERJEE and A. A. JOHNSON, *Mater. Sci. Engng* **11** (1973) 283.
7. T. TADAKI, Y. NAKATA, K. SHIMIZU and K. OTSUKA, private communication.
8. J. KWARCIAK, Z. LEKSTON and H. MORAWIEC, *J. Mater. Sci.* **22** (1987) 2341.
9. G. BENSMANN, F. BAUMGART and J. HARTWIG, *Tech. Mitt. Krupp* **37** (1979) 21.
10. S. MIYAZAKI, K. OTSUKA, *Metall. Trans. A* **17** (1986) 53.
11. V. N. HACIN, J. I. PASCAL and V. E. GIUNTER, *Fiz. Met. Metallov.* **46** (1978) 511.

Received 20 July 1987
and accepted 28 April 1988